

3D models and structural analysis of rock avalanche: deformation process during the propagation mechanisms

Answers to Referees

Dear Reviewers, each of your comments are answered in details below:

Referee #1

Comment 1: Equifinality of structural features is a problem. The occurrence of the same structural features in both, friction-controlled laboratory-scale granular flows and highly mobile, dynamically fragmenting rock avalanches simply implies some fundamental and intrinsic behaviour of all granular masses in motion. It does not, however, elucidate the long-runout characteristic of large rock avalanches, and thus limits the extrapolation of dynamic processes from the lab to the field significantly. I would therefore suggest that the authors emphasize that deformations not dynamics are investigated through their methods.

Answer: we thank you the referee for this useful comment. We will then stretch out that the main objective of this research is to propose tools and work-flow to rapidly map the features present at the surface of deposits. These features provide important information on the mobility of the rock avalanche. The method was first tested within our laboratory results of dry granular flow where we highlighted deformation process then we applied it to real case event, the Frank Slide for this study.

Changes in manuscript: The manuscript will be changed in order to clarify the fact that we attempt to propose a simple methodology to describe the features at the surface, not to improve our understanding for the process generating the long runout of rock avalanches. Moreover, we will be more precise in the fact that we emphasize the deformations and not the dynamic. The title of the paper will also be changed to be clearer.

Comment 2: No scaling calculations were applied, which is a prerequisite if dynamics are to be compared to phenomena of different scales. This could have furthermore, a priori, solved the problem of grain sizes being too large to capture the deformation features (the scale of which is known from previous experiments of this kind, which should be cited more comprehensively).

Answer: The authors are aware that no scaling calculations were applied as we do not attempted to propose a real dynamic interpretation but we based our value for the laboratory on previous work to be in the interval of the scaling. As the referee suggest, we will underline better the purpose of this study, as stated in the previous comment to avoid misunderstanding.

Changes in manuscript: Some scaling values obtained by previous authors will be reported in the manuscript. Consideration about grainsize ration will also be added to the text.

Comment 3: How do the authors explain that mixing between stratigraphic units is observed in the laboratory but not in the field?

Answer: In laboratory, loose material is use involving a partial mixing of the grains. The fragmentation of the layers is not taken into account whereas it plays a role in the field.

Changes in manuscript: A sentence will be added about the mixing in order to clarify this difference with real cases.

Comment 4: The authors should clearly state how (if) their analogue models differ from the many done before and how (if) their analysis technique adds new merit or better insights or easier/cheaper/faster application or more detailed results. a. How does their technique differ from other analyses tools of surface roughness etc.? b. Is the code freely available? c. Who has done such experiments before (in addition to the few papers cited) and how do their results compare?

Answer: according to the referee we will enlarge our bibliography and underline the difference between our works and the works of other authors. The analysis technique based on the filters is easy and fast (around 2h for the experiments + point clouds reconstruction + filtering). It is also cheap as you only need a camera to take pictures. In our study we used the softwares Agisoft Photoscan and Polyworks to construct the 3D point cloud and Matlab for the filtering. Some softwares are freely available, as Cloud Compare and Visual SFM for the point clouds and Octave instead of Matlab. By using these softwares, our method becomes even cheaper.

- a) References about the surface roughness will be added to the text.
- b) I will discuss with the coauthors about the free access to the code.
- c) Here again, references will be added

Changes in manuscript: according to the suggestion of the referee we will improve our manuscript adding in the description of the method some statements regarding the fact that it is fast and easy to use as well as cheap. Some other references will also be added to the text for the roughness and experiments in order to compare the results.

Specific Comments: we thank the referee for the useful comments which will certainly integrate in the text and which will improve the quality of the paper and put in evidence the importance of the present work.

Referee #2

Comment 1: Introduction is quite broad but relatively limited in the presentation of similar modeling approaches. A slightly more complete and updated review could result in a more useful or general overview. The description of large scale features in real landslides could be useful but it is not a primary point to consider.

Answer: This point was also highlighted by referee 1 and the authors agree with this comment. The introduction will be completed.

Changes in manuscript: modeling approach will be updated in the introduction

Comment 2: Data acquisition: probably this paragraph could be titled Methods or experimental methods.

Answer: Thanks for the suggestion, the change will be done.

Changes in manuscript: this paragraph will be called "experimental methods"

Comment 3: I am not sure which kind of material has been adopted but probably carborundum (not carborandum) or silicon carbide. This is a particular material characterized by high density and very low friction. This is a major point that would be useful to evaluate because there is no description of the material properties, both in terms of internal friction angle and of basal friction angle/coefficient. As a consequence, the interpretation and possible reuse of the experimental data by other researchers would require a basic characterization or at least the reporting of literature or technical data

Answer: Thanks for noticing the "carborandum" typo; it will be corrected in the manuscript. A better characterization of the material will be proposed. Measurements of friction angle and

basal friction will be carried out in our laboratory and included in the text. Concerning the electrostatic effect, different experiments were carried in our lab about that and the publication is in prep.

Changes in manuscript: The “carborandum” mistake will be corrected; a better description of the carborundum will be proposed.

Comment 4: Dimensional analysis could be named or considered even if most of the scaling laws and dimensionless number have been already reported in the literature. Some mention or value could be given or simply report the variables values so to allow for a computation of the numbers.

Answer: As answered for Referee 1, no dimensional analysis was carried for this study but we based our values on number of literature.

Changes in manuscript: Some scaling values obtained by previous authors will be reported in the manuscript.

Comment 5: The problem of the electrostatic effects could be relevant considered the extremely small mass/volume of material adopted in the tests. A more specific description of carborundum is required also on this basis.

Answer: we will add the electrostatic effect within the description of the carborundum as proposed in comment 3.

Comment 6: For the colored granular material and for a better understanding of the possible processes and structures, it would be useful to know the material properties of the colored sands at least to evaluate the differences and for possible use by other researchers.

Answer: As for the carborundum, measurements of friction angle and basal friction will be carried out in our laboratory

Changes in manuscript: a better description of the color sand will be added to the manuscript.

Comment 7: Study of the effects of roughness is an interesting aspect of this research. At the same time it is not common to compare this to realistic conditions where usually roughness is no a fixed bed condition. In fact, most of the times the basal surface is naturally rough but is also erodible (i.e. not fixed).

Answer: Indeed, our roughness is not realistic compared to realistic conditions but it gives good insight of how the basal roughness influences the motion of the propagation. To simulate the roughness with erodible basal surface could be interesting for further studies.

Changes in manuscript: A comment on this will be added in the text.

Comment 8: Fixing slope angle to 40° is reasonable but at the same time neglect to study the relevance of slope angle in controlling flow evolution and deposition.

Answer: The influence of the slope angle on the flow evolution and deposition is the object of a future publication. Nevertheless, few lines about the slope influence can be added to this research to clarify the influence, referring to other authors.

Changes in manuscript: Few lines will be added about the slope influence

Comment 9: The relevance for counting the number of colored grains within a specific area should be explained more.

Answer:

Changes in manuscript: few lines will be added to clarify this point.

Comment 10: Methods: again, the type of system adopted for the acquisition should be better detailed. For example, the number of fps for the high speed camera, or the resolution and precision of the laser scanner.

Answer:

Changes in manuscript: Some complementary information about the data acquisition will be added to the text.

Comment 11: Sfm is introduced in quite a general way but then is dismissed by simply saying that is not relevant because does not work with this kind of material. So there is no mean at introducing it. Light scattering at the grain surface could also be a problem with laser scanning and so this could be mentioned or at least it should be said if really important considering the scale of the problem. This point is partially tackled but not clearly stated.

Answer: For other study we carried in our laboratory (paper in prep.), no problems of reflection were observed when using carborundum, contrary to the photogrammetry that result into a noisy point cloud when it is scanned by the Lidar. For this reason, we applied photogrammetry to the colored sand. The advantage of the photogrammetry with the colored sand is that we have a colored point cloud and way more point compare to the Lidar. On the other hand, acquisition with the Lidar allowed us to have point clouds of all experiments carried out with carborundum. We attempted to adapt the method for different situations. Moreover, the SfM is cheaper compare to Lidar.

Changes in manuscript: Precisions and a better comparison of the two techniques will be provided in the text.

Comment 12: Gradient operator filtering: not novel per se, but anyway it is found useful to the aim of the study and helps in a clearer definition of the structures.

Answer: Thanks for the comment. Indeed the filtering helps in a clearer definition of the sturctures. In order to highlighted how our method is useful (cheaper, faster and easy to use), some comments will be added in our manuscript and compared to other methods.

Changes in manuscript:

Comment 13: Visual inspection: I have to admit that from the figures the internal structures are extremely difficult to be seen and recognized. At the same time, the authors should describe a little bit more the role or effects of different materials, of the friction characteristics of the involved materials.

Answer:

Changes in manuscript: As previously discuss, characterization of the material will be add to the manuscript. However, some complementary description of the figure of the visual inspection will be added taking into account the role and effects of the different materials. For the figure, we will try to make it clearer.

Comment 14: High speed videos: the general quality of the images is low and this could be simply a problem of the uploaded file resolution. Nevertheless, apart for the colors the general evolution is poorly constrained. The reason for passing from carborundum to sand should also explain at least to clarify the possible effects. For example, why in this case there is no attention to the electrostatic effects named at the beginning for the adoption of carborundum?

Answer: For the high speed camera, we had to find the better compromised with resolution and fps. Indeed, with more fps, the resolution decreases. Nevertheless, it may be a problem within the uploading file, it has to be controlled and adjust. The reason for passing from carborundum to colored sand is due to the problem with the method used as it has been explained in the text and in comment 11.

Changes in manuscript: Few lines will be added in addition to those of the comment 11 about electrostatic effects and on the reasons of the choice of the different materials

Comment 15: Frank slide: probably is too much to introduce the Frank slide example as it is in the manuscript, considering the length of the description (just a few lines).

Answer:

Changes in manuscript: the description of the Frank Slide has been moved to the chapter now called "experimental methods".

Comment 16: Discussion: there is some interpretation in terms of time for the formation of the internal features. It should be clear that there is no real observation in time for the formation of the internal features. So talking about a possible order of formation is at least improper. The same could be said about the significance of these features about the flow.

Answer: we thank the referee for this comment and we agree on it, after this we decided not to include an interpretation of the formation of the internal features/time because it is not possible in the framework of our study

Changes in manuscript: The figure 13 will be removed

Comment 17: In the description of flow and formation of structures I think it should be carefully considered how a flow in extensional regime could be at the same time exerting a compressional action. In a certain way this seems not possible unless a clearer explanation is given (see e.g. step 6 in the sequence).

Answer:

Changes in manuscript: the description will be cleared in the manuscript

Comment 18: The effect of the layering (transversal to the release geometry) should be mentioned.

Answer:

Changes in manuscript: this layering effect will be added to the text.

Comment 19: As said above the internal structures do not seem to be so clearly recognizable. Furthermore, if the material in the tail is slower and much slower than the frontal part it is unclear how the pushing action is occurring.

Answer:

Changes in manuscript: A more detailed description has been added to the text in order to clarify it.

Comment 20: The various steps are in a certain way re- expressed in the successive list of points when internal structures are described - Point 1 in the discussion: the velocity at the front is assumed similar to the one at the back: is this possible or realistic considering that thickness is different, no pressure contribution is present and that the tail motion is lasting more?

Answer: As said in the answer to the comment 16, we decided to remove the figure 13 as the internal deformation can not be interpreted in our study

Changes in manuscript:

Comment 21: It is said that it is possible to understand now why the structures are not randomly distributed. Actually, no one ever said that they are or should be randomly distributed; on the opposite it is clear that there is a reason for the general disposition and order of formation.

Answer: we agree with the referee that the sentence could be misleading, we should say that our study confirm that the structures are not randomly distributed and that there is a similarity of the distribution between laboratory and real cases.

Changes in manuscript: sentences will be rewritten in order to avoid any misunderstanding about this point.

Comment 22: Referencing: I suggest to complete a search for granular flow modeling considering some interesting laboratory results about the propagation along slopes, on hard or soft layers with different characteristics and the description of internal structures or formation of lateral levees as delimited by sort of strike slip features. Some other piece of research describes the evolution in time of granular flows during their motion and deposition. Since older works from Gray to more recent ones. An interesting one has been published by Rowley et al., 2001 and more in recent papers.

Answer: we agree with these comments and we will expand our bibliography.

Changes in manuscript: new references will be added to the text and the introduction and the discussion will be changed accordingly.

3D models and structural analysis of ~~analogue granular deposits~~ rock avalanche: a kinematic analysis the study of the deformation process to better understand the propagation mechanism

C. Longchamp¹, A. Abellan¹, M. Jaboyedoff¹ and I. Manzella²

[1]{Institute of Earth Sciences, University of Lausanne, Switzerland}

[2]{Department of Earth Sciences, University of Geneva, Switzerland}

Correspondence to: C. Longchamp (celine.longchamp@unil.ch)

Abstract

Rock avalanches are extremely destructive and uncontrollable events that involve a great volume of material ($>10^6 \text{ m}^3$), several complex processes and they are difficult to witness. For this reason the study of these phenomena using analogue modelling and the accurate analysis of deposit structures and features of laboratory data and historic events become of great importance in the understanding of their behavior.

The main objective of this research is to analyze rock avalanche dynamics and deformation process by means of a detailed structural analysis of the deposits coming from data of 3D measurements of mass movements of different magnitudes, from decimeter level scale laboratory experiments to well-studied rock avalanches of several square kilometers magnitude.

Laboratory experiments were performed on a tilting plane on which a certain amount of a well-defined granular material is released, propagates and finally stops on a horizontal surface. The 3D geometrical model of the deposit is then obtained using either a scan made with a 3D digitizer (Konica Minolta vivid 9i) either using a photogrammetric method called Structure-from-Motion (SfM) which requires taking several pictures from different point of view of the object to be modeled.

In order to emphasize and better detect the fault structures present in the deposits, we applied a median filter with different moving windows sizes (from 3x3 to 9x9 nearest neighbors) to the 3D datasets and a gradient operator along the direction of propagation.

1 The application of these filters on the datasets results in: (1) a precise mapping of the
2 longitudinal and transversal displacement features observed at the surface of the deposits; and
3 (2) a more accurate interpretation of the relative movements along the deposit (i.e. normal,
4 strike-slip, inverse faults) by using cross-sections. Results shows how the use of filtering
5 techniques reveal disguised features in the original point cloud and that similar displacement
6 patterns are observable both in the laboratory simulation and in the real scale avalanche,
7 regardless the size of the avalanche. Furthermore, we observed how different structural
8 features including transversal fractures and folding patterns tend to show a constant
9 wavelength proportional to the size of the avalanche event.

10

11 **1 Introduction**

12 Rock avalanches, or Sturzstroms (Heim, 1932) are defined as an extremely rapid, massive,
13 flow-like motion of fragmented rocks derived from a bed-rock failure (Hungar et al., 2001).
14 Rock avalanches are events in which granular masses of rock debris flow at high speeds,
15 commonly with unusually runout (Corominas, 1996; Friedmann and Losert, 2003). A great
16 volume of material ($>10^6 \text{ m}^3$) is involved and the flowing mass can reach velocities in the
17 order of tens meters per second. They can travel long distances, in the order of kilometers and
18 cover an area over 0.1 km^2 (Hsü, 1975). They present a very high mobility and need to be
19 simulated with adapted frictional models (Hungar et al., 2001, Pedrazzini et al., 2012). Authors
20 proposed different possible causes , which could explain the high mobility of these
21 phenomena, such as the influence of the large destabilized volume (Heim, 1932; Hsü, 1975;
22 Scheidegger, 1973; Nicoletti and Sorriso-Valvo, 1991), the momentum transfer within the
23 rear and the front of the flowing mass (Van Gassen and Cruden, 1989; Manzella and
24 Labiouse, 2009), or the fragmentation of the spreading mass (Heim, 1932; Davies, 1982;
25 Davies and McSaveney, 1999; Locat et al., 2006). In order to understand the behavior of such
26 granular flows, laboratory scale experiments provide important information on their
27 propagation and on the parameters influencing their mobility, even if they reproduce idealized
28 conditions (Davies and McSaveney, 1999, 2003; McDougall and Hungar, 2004; Shea and van
29 Wyk de Vries, 2008; Manzella and Labiouse, 2008, 2009; [Longchamp 2016](#)). [Dufresne](#)
30 [\(2012\) highlighted that substrate material with the least frictional resistance showed the](#)
31 [greatest response to granular flow, producing the longest runout. In their work, Andrade et al.](#)
32 [\(2010\) and Paguican et al. \(2014\) studied analogue flank collapse and highlighted that](#)

1 | hummocks can form horst and graben structures during lateral spreading. Several authors
2 | proposed different parameters for the geometrical description of large landslides. One of the
3 | most used is the Fahrböschung concept, which was introduced by Heim (1932) to estimate the
4 | maximum runout of rock avalanches or landslides (Scheidegger, 1973; Hsü, 1975; Davies,
5 | 1982) and which is defined as the angle of the straight line connecting the head of the scar to
6 | the end of the deposit.

7 | The presence of faults and folds are common features on the surface of rock-avalanche
8 | deposits. One of the best examples is the rock avalanche deposit of Socompa volcano
9 | (Northern Chili). This deposit was widely studied before (Francis et al., 1985; van Wyk de
10 | Vries et al., 2001; Kelfoun and Druitt, 2005; Shea and van Wyk de Vries, 2008) and presents
11 | a well preserved morphology thanks to the local arid climate. A complex assemblage of
12 | surface structures (normal faults, strike-slip faults, thrusts, ridges) is displayed on the surface
13 | of the deposit. Van Wyk de Vries et al. (2001) showed that these structures incise deeply the
14 | internal part of the deposit. The non-volcanic deposit of Blackhawk (California, USA) also
15 | presents similar features (Shea and van Wyk de Vries, 2008) (Figure 1a) as well as the Frank
16 | Slide in Alberta (Canada) (Cruden and Huger, 1986, 2011; Charrière et al., 2015). Features
17 | perpendicular to the flow direction are mainly present in the distal part of the deposit and are
18 | interpreted as the surface expression of the underneath topography. Reversibly, longitudinal
19 | features on the proximal and the central part of the deposit are assumed to be morphological
20 | features that were created during the process of avalanche propagation and deposition. It is
21 | also interesting to highlight that similar features have been observed in other planets such as
22 | in the Mont Olympus (Mars) (Figure 1b). Shea and van Wyk de Vries (2008) provided a
23 | detailed map of this extraterrestrial Martian rockslide avalanche where it can be observed that
24 | thrust faults are located in the front of the deposit and that are cut by strike-slip faults. Normal
25 | faults are presented in the central part of the deposit. Although, these features occur during
26 | the emplacement of the deposit, however, few studies focus on these deformational settings.

27 | In their small-scaled experiments, Dufresne and Davies (2008) showed that lateral levees
28 | developed where flows was parallel to the confining whereas compressional ridge formed in
29 | response to declination in the front of the deposit.

30 | In the present paper a detailed structural analysis is carried out based on data coming from
31 | dedicated laboratory experiments and historic events in order to better understand the
32 | dynamics-deformation of these complex phenomena. Moreover, this research attempted to

1 propose a simple methodology to describe and map the features at the surface of the deposits
2 in order to provide information on the mobility of the rock avalanche.

3 **2 Data acquisition**Experimental methods

4 The first step of this study consisted in carrying out laboratory experiments in order to study
5 the influence of a series of parameters on the features and structure of granular flow deposits.

6 The experimental setup (see Figure 2) consisted in a simple ~~aluminium~~aluminum slope
7 geometry composed of two distinct parts: a 90 x 70 cm slope with an inclination (α) which
8 can be precisely modified, connected with a curved part to a 120 cm long horizontal surface.

9 Furthermore, the experimental setup also includes a box (11 x 8 x 7 cm) where the loose
10 material is enclosed at the beginning of the experiment. This box, separated from the main
11 set-up, can be leant against the slope and quickly separated from it by means of a retractile
12 jack. This allows placing a precise quantity of granular material on the slope and
13 ~~realising~~releasing it avoiding any vibrations. Experiments then consist letting the mass
14 propagating without lateral confinements till it reaches a complete stop (Figure 2). As loose
15 material is used, partial mixing of grains is observed. The fragmentation of layers is not taken
16 into account in this study.

17 Two different materials were used for the experiments: a) the first type of material
18 corresponds to angular and calibrated ~~carborandum~~carborundum sand (SiC, density = 3.21
19 g/cm³) with three different grainsizes (Table 1). The choice of ~~carborandum~~carborundum was
20 made in order to avoid the characteristic electrostatic effects that have been often observed in
21 granular flow experiments and that are not present in real events (Iverson and Denlinger 2001;
22 Manzella, 2008). Furthermore, the angular shape of this type of material has close
23 resemblances with natural material; b) the second material corresponds to colored sands of
24 similar grainsize (Table 1). The choice of this material was driven by the need of observing
25 the evolution of the initial stratigraphy, i.e. to analyze the deposit stratigraphy (given by
26 different layers of different colors) during motion and emplacement of the mass.

27 The slope and the surface of deposition were artificially roughed by adding sandpaper, also
28 made of ~~carborandum~~carborundum sand, where the grain diameter has been varied. ~~The basal~~
29 ~~roughness R_a has been deduced according to the formula of Adams et al. (2012) and shown in~~
30 ~~equation 1:~~

1 ~~$\epsilon = 5.863Ra$ (1)~~

2 ~~where Ra [μm] is the roughness of a hypothetical surface assumed to be made of a uniform~~
3 ~~monolayer of spheres having the same mean diameter c [μm].~~

4 ~~Based on equation 1, the basal roughness Ra can be calculated as follow (equation 2):~~

5 ~~$$Ra = \frac{\epsilon}{5.863}$$~~

6 ~~(2)The basal friction μ angle for each sandpaper was estimated by means of a dynamometer~~
7 ~~and the results are given in Table 2.~~

8
9 ~~The basal roughness Ra varied between $45.88 \mu\text{m}$ ($c = 269 \mu\text{m}$) (for the coarser sandpaper)~~
10 ~~and $1.43 \mu\text{m}$ ($c = 8.4 \mu\text{m}$) (for the finer sandpaper) to obtain six different substrata (Table 2).~~

11 ~~No scaling calculations were applied for this work but we based our value for the slope,~~
12 ~~height of fall grainsize for the laboratory on work of Shea and van Wyk de Vries (2008). All~~
13 ~~the experiments were carried out with a constant volume within the same experiment (400cm^3~~
14 ~~$< V < 500\text{cm}^3$), same slope angle (40°) and same height of fall for the granular material (50~~
15 ~~cm). The runout of dry granular flow is influenced by the slope angle: the runout distance is~~
16 ~~greater for higher slope angle (Longchamp, 2016). For this study, a slope angle of 40° is~~
17 ~~chosen to better compare the results.~~

18 The experiments were recorded by a high speed camera (30 fps for a resolution of 640x480),
19 the final deposit was scanned by a 3D digitizer (Konica Minolta vivid 9i micro-Lidar with a
20 resolution of 30'000 points per point cloud, Figure 2) and photographed. Finally a transparent
21 separation is placed carefully along the major longitudinal section and the material on one
22 side is removed so that it is possible to observe the internal structure of the mass. In order to
23 observe the repartition of the colored sand grains within the deposit, sand grains were counted
24 at crucial sections along the deposit. For each measurement, a section of 0.2 cm length and a
25 height corresponding to the thickness of the deposit was determined. Into this section, the
26 number of colored grains was manually counted. This gave further information on the
27 different regimes affecting the flow and allowed to better constrain the different part of the
28 deposit that are affected by different regime. Ten measurements were made along the deposit
29 and cumulated.

1 In order to have significant results, three experiments are carried out with equal initial
2 conditions.

3

4 **3 Methodology**

5 As mentioned above, during the propagation, the motion of the granular mass is recorded by a
6 high-speed camera in order to analyze the deformation and spreading during the flow. Once
7 the mass stopped, the first step was to take pictures of the deposit in order to study and
8 inventory the visible longitudinal and transversal features on the surface. The acquisition of
9 3D dataset was made using either a laser scanner (Konica Minolta vivid 9i micro-Lidar) either
10 a photogrammetry technique, named Structure-from-Motion (SfM) (Westboy, 2012). The
11 laser scanner technique is useful to scan the deposit resulting of the propagation of
12 ~~carborandum-carborundum~~ sand but the density of points is quite low (30'000 points per point
13 cloud) (see Figure 3b). Moreover, the setup is quite difficult to install and the data are long to
14 process. SfM differs fundamentally from conventional photogrammetry, in that the geometry
15 of the scene, camera positions and orientation is solved automatically without the need to
16 specify a priori a network of targets which have known 3-D positions (Westboy, 2012).
17 Instead, these parameters are solved simultaneously using a highly redundant, iterative bundle
18 adjustment procedure, based on a database of features automatically extracted from a set of
19 multiple overlapping images (Westboy, 2012). Structure from Motion is a simple technique
20 requiring little material and is cheaper compare to Lidar. The density of points is high
21 (1'000'000 points per point cloud). This density of points allows identifying finer features on
22 the deposit. The main disadvantage of this technique is that the post processing of the data is
23 sensitive to all variation in the images. Therefore, SfM cannot be applied to experiments with
24 ~~carborandum-carborundum~~ sand as the grains reflect the light with different intensity
25 according to where the pictures is taken and it could only be applied to the colored sand
26 deposit (Figures 4). To summarized, no problems of reflection were observed when using
27 carborundum when it is scanned by a Lidar. On the contrary, when using photogrammetry on
28 the carborundun sand, the resulting point cloud is noisy. For this reason, we applied the
29 photogrammetry to the colored sand. The advantage of the photogrammetry with the colored
30 sand is that we have a colored point cloud and way more point compare to the Lidar. On the
31 other hand, acquisition with the Lidar allowed us to have point clouds of all experiments
32 carried out with carborundum. Thanks to the use of different filtering techniques and

1 operators, we were able to highlight the structural fingerprints on the deposit surface. This
2 computational work aimed to highlight the features that cannot be observed by a naked eye, as
3 follow:

4 (a) Application of a median filter technique

5 Data acquisition using 3D digitizer leads or SfM to a “noisy” surface in which the features to
6 be detected are masked due to the scattering of the 3D points around the real surface (Figure
7 5a). To remove the noise, smoothing filters are used in preprocessing steps (Gonzalez and
8 Woods, 2002; Pugazhenti and Priya, 2013). After Gonzalez and Woods (2002), order-statistic
9 filters are nonlinear filters whose response is based on ordering the pixel contained in the
10 image area encompassed by the filter, and then replacing the value of the center pixel with the
11 value determined by the ranking value. The first step was to remove the noise using a 2-D
12 median filtering using different window sizes (Figures 5b and 5c).

13 (b) Application of a gradient operator

14 Once the noise was removed of the dataset obtained with 3D digitizer or SfM, a numerical
15 gradient is applied to the filtered dataset. The gradient was applied along two directions to
16 highlight changes in the slope orientation as proposed in Kumar et al. (1996) and Gonzalez
17 and Woods (2002). First, we calculated the gradient parallel to the flow direction (along the x
18 axis), and then the gradient perpendicular to the flow direction (along the y axis):

19
$$\nabla F = \frac{\partial F}{\partial x} i + \frac{\partial F}{\partial y} j \quad [3]$$

20 The objective of detecting variation of the gradient along x and y is to highlight any
21 preferential orientation. The detected variations of the slope are interpreted as structures
22 developed on the surface of the deposit. Once the gradient operator is applied, the point cloud
23 is imported in the IMInspect module of Polyworks software (InnovMetric)

24 (c) Comparison with real case

25 In order to extend the proposed workflow to a real case study, we decided to apply the
26 filtering gradient operator techniques to the well-known Frank Slide event (Alberta, Canada).
27 This deposit presents several geometrical features, which are mainly longitudinal and
28 perpendicular to the flow direction (Longchamp et al., 2011; Charrière et al., 2015).

1

2 **4 Results**

3 **4.1 Results I: Experiment description**

4 **a) Visual inspection from photography**

5 Laboratory experiments were carried out with different volumes, grainsizes and using
6 different basal roughness but only the finer grainsize (F120) presented visible features on the
7 surface of the deposit as shown in Figure 6a. Three distinct sets of features can be observed in
8 this figure: inverse faults, normal faults and strike-slip faults. The first set, the inverse faults,
9 is composed of long features, perpendicular to flow direction following the outline of the
10 front with a tendency to become parallel to the global flow direction at the lateral margins
11 (green lines on Figure 6b). The second set is formed by thin normal faults located at the rear
12 part of the deposit and perpendicular to the flow direction (red lines on Figure 6b). Two
13 different sets of strike-slip faults can be observed. The first one is composed of short and thin
14 features parallel to the flow direction and present at the front of the deposit. These features
15 can be observed cutting the inverse faults at the frontal part and cutting the normal faults at
16 the rear part. The second one is made of strike-slip faults parallel to the flow direction and are
17 present at the lateral margins of the deposit.

18 **b) Visual inspection from high speed video**

19 In high-speed video, propagation of the mass is easily observable. Sand of three different
20 colors was used and was poured in the starting box as follow: 150 ml of red sand as the lower
21 layer, 150 ml of grey sand as intermediate layer and finally, 150 ml of green sand. The slope
22 is made rough with the finer substratum ($\mu=33.40^\circ Ra=1.43\text{-}\mu\text{m}$) and the slope angle is 40° .
23 Once the trap is open and the material is free to flow, all the layers are stretched under an
24 extensional regime. Once the frontal part reach the horizontal surface, its velocity is
25 decreased. As the mass continues to flow on the slope, the front is compressed and pushed
26 forward. The mass is finally stopped once all the mass reaches the horizontal surface. The
27 high-speed video is available in supplemental material.

4.2 Results II: point cloud processing

Figure 7 shows the results of the point cloud processing for all the simulations, i.e. using three grainsizes (F10, F36 and F120) on the different substrata (Table 2). For the coarser grainsize (F10), the application of the different filters and operator techniques has not highlighted any remarkable features. As the amplitude of the features is less than one millimeter, the coarser grainsizes are too large to capture deformation. The only noticeable thing is that the shape of the deposit became more ellipsoidal with a decreasing basal roughness and confirmed the observation made by Dufresne et al. (2016) that substrates shaped the morphology of rock avalanches. For the medium grainsize (F36) the filters clearly highlighted a series of features perpendicular to the flow direction. ~~The density of these features increases with the reduction of the basal roughness. In this case filters allowed detecting features that were not visible on the pictures alone.~~ In Figure 7, it also can be observed that the basal friction influenced the formation of features at the deposit surface. The density of these features increases with the reduction of the basal roughness. In this case filters allowed detecting features that were not visible on the pictures alone.

As it can be observed on Figure 7, the gradient along Y can be considered as an efficient manner for the observation of the different features affecting the surface of the deposits.

Using this operator, we observed that the back of the deposit presents high concentration of small features parallel to the flow direction. Figures 8a and 8b present the back of an analogue deposit (F120 on the finest substratum) after the point cloud processing and imported in the IMInspect module of Polyworks software (InnovMetric). Two different sets are observable: one perpendicular to the flow direction and the second composed of features parallel to the flow direction and cutting the first set (Figure 8). The first set was observed with naked eye whereas the second set is only recognizable after post processing.

4.3 Frank Slide

The same visual inspection and filtering methods were applied to the Frank Slide deposit. Figure 9a is the result of the interpretation of the features mapped directly on the DEM and Figure 9b is the result of the application of a gradient along the flow direction. The main features observed in the DEM are also recognizable on the gradient map, but a series of structures that are masked on the DEM image can be identified in the gradient image. Figures 9c and 9d show a zoom of the deposit after the filtering. In the Figure 9c, features parallel to

1 the flow direction are clearly identifiable whereas in the Figure 9d, the features are parallel to
2 the flow direction.

3 **5 Discussion**

4 Our workflow has allowed the identification of three distinct sets of features on the analogue
5 granular flow deposit. Those features are important marks of the processes happening during
6 the flow and the emplacement of the mass and could be crucial in improving our
7 understanding of the dynamics and the reasons of the high mobility of rock avalanches. The
8 inverse faults are well marked on the deposit front, reflecting the compression affecting the
9 frontal part of the mass. Inverse faulting system appears as soon as the frontal part of the
10 granular mass hits the surface of deposition and its velocity starts to slow down. Then, the
11 granular material accumulates on the rear part, pushing forward and compressing the frontal
12 part of the deposit. Normal faults were formed during an extensional regime, when the mass
13 was stretched during the flow and by the pulling of the frontal part of the mass. Strike-slip
14 faults are present at the front of the deposit. As the mass is thinner at the margins and
15 consequently the velocity decreases while the central part of the mass is still on motion letting
16 strike-slip faults appear at the lateral margins of the deposit. The strike-slip faults are the
17 expression of the shearing occurred during the deceleration of the mass (Shea and van Wyk
18 de Vries, 2008).

19 Thanks to the application of the filtering on analogue deposit 3D datasets, the structures
20 observed during the laboratory experiments were highlighted. One advantage is that the use of
21 filters allows detecting features for the finest sand (F120) and also for the medium one (F36),
22 for the totality of the basal roughness. The fact that no features are observed for the coarse
23 grain size (F10) can be explained by the fact that the size of features is of the same order of
24 magnitude that the size of the grains. The gradient along Y gave the best results since it
25 allowed detecting long inverse faults at the front and some normal faults at the back.
26 Moreover, the study of the result of the Y-gradient with the Polyworks software shows that
27 the normal faults at the back are numerous and cut by strike-slip faults (Figure 8). These
28 strike-slip faults appear after the extensional regime, during the shearing caused by the mass
29 deceleration. These features give crucial information for the mobility of the mass and are not
30 detectable with naked eye.

31 Thus, different regimes were distinguished: the compressional, the extensional and the
32 shearing regimes. Based on this assumption we could deduce the behavior of the granular

1 mass looking at the high-speed camera snapshots as shown in Figure 10. This figure
2 represents for each time step on one side the movie snapshot and on the other the
3 interpretation related to it. In order to improve the clarity of the observation made, no
4 distinction between the layers is made for the interpretation. Two main regimes are detected,
5 the compressional, outlined on the interpretation with dots and the extensional one, outlined
6 with lines. Following the time steps shown in Figure 10 we can then observe:

7 Step 1: Once the trap is open, the front of the granular material starts to flow. Because of the
8 release geometry, layering occurred during the flow.

9 Step.2: All the mass behaves under an extensional regime through all directions during the
10 time preceding the deposition of the granular flow.

11 Step.3: Shortly after the free flow, the front of the mass hits the surface of deposition,
12 decreasing suddenly its velocity. Two different tensional states are found at this step.
13 While the mass on the slope it is under high extensional regime the front starts to be
14 under compressional regime as it hits the surface of deposition and the velocity starts
15 to slow down. In addition to that, at this stage of the experiment, we start observing
16 one additional aspect characterizing the green layer. In fact we can first distinguish a
17 part of the green mass flowing which behaves differently from the rest of the mass.
18 This part is likely to constitute the rear zone in the initial configuration of this layer.
19 Moreover, at this step, it can be observed that the basal red layer has a lower velocity
20 than the other layers, as it is less visible in the picture.

21 Step.4: At this step, the back is still under an extensional ~~regime~~and regime and the front
22 under a high compressive regime as the flowing material continues to push it
23 forward. The rear part of the green layer is faster than the underneath layers.

24 Step.5: The gray and green layers continue to be pushed by the main body of the mass.
25 Consequently, shearing appears at the front. As the red layer is the basal layer, it is
26 slowed by friction. As the margins of the mass are thinner compared to the central
27 part, their velocity is less important and shearing takes place. Simultaneously, the
28 rear part of the green layer is faster compare to the lower layers and hits the mass
29 already deposited.

1 Step.6: The back of the mass continues to flow and is still under extensional regime, pushing
2 the front forward. At this step, shearing is still important at the margins and at the
3 front.

4 Step.7: The front is stopped and the rest of the material still on the ramp finishes to flow down
5 creating the shearing observed at the back of the deposit, cutting the normal faults.

6 Step.8: The mass is finally stopped. It is interesting to highlight that the original stratigraphy
7 is conserved and observable at the front.

8 The profile AA' along the flow direction was obtained for the laboratory experiment (Figure
9 11a). This profile allowed observing the internal part of the mass and the depth of the main
10 features. Figure 11b gives the image of the section along the AA' line shown in Figure 11a
11 and the Figure 11c is its interpretation. In Figure 11c, inverse faults are visible at the front
12 (well-marked by red grains in the Figure 11b) whereas normal faults are visible at the rear
13 part of the deposit. In this figure, it can be observed that the center of the mass is mainly
14 composed of green sand, confirming that the rear part of the green layer in Figure 10 hits the
15 mass already present on the surface of deposition (steps 5-7 in Figure 10). When this mass
16 hits the deposit, it probably increased the compression explaining the numerous inverse faults
17 present at the front (Figure 11c).

18 To confirm what observed the number of colored sand grains has been counted along the
19 central section of the deposit, as reported on Figure 12. Results confirmed what showed by
20 Figure 11b and 11c with the identification of an extension-dominated area in the rear and a
21 compression dominated area in the front. The rear part of the deposit corresponds to the
22 extension-dominated area. This area is mainly composed of red sand whereas few green
23 grains were observed. In the contrary, the central part of the deposit is mainly composed of
24 green sands. Indeed, this part corresponds to the rear part of the deposit that hit the mass
25 already deposited (Figure 10). The frontal part of the deposit corresponds to the compression-
26 dominated area. The compression caused by the impact of the green layer of grains in the
27 central part pushed part of the lower layer (red) further on the front and towards the surface
28 creating the inverse faults also showed in Figure 11c. Indeed, in this frontal part, we can
29 observe that the amount of red sand increases.

30 Because of the position of the profile, the red layer is not clearly visible at the front of Fig.
31 11b and 11c but the conservation of the initial stratigraphy is observable in the Fig. 11a. The
32 fact that the initial stratigraphy is preserved in the final deposit it is relevant since this feature

1 has been already detected in several real cases and it has been recognized as one of the main
2 ones characterizing rock avalanche deposit (Erismann, 1979, Manzella and Labiouse, 2013).
3 Thanks to the film analysis we could then relate some propagation mechanisms with the
4 consequent preservation of the initial stratigraphy in the final deposit and this could give an
5 insight in the dynamics of real rock avalanches.

6 ~~Based on these observations, we can propose a mechanism of propagation of a granular flow
7 as shown in Figure 13 and explained in the following:~~

8 ~~1. The granular material is released and the extension of the mass starts immediately when the
9 mass starts to flow. When the mass flows freely on the slope, the velocity of the front is
10 assumed to be similar to the velocity observed at the back of the moving mass (Shae and
11 van Wyk de Vries, 2008).~~

12 ~~2. When the front of the mass hits the horizontal surface, a compressional regime appears at
13 the front while the mass on the slope is under high extensional regime. The frontal part of
14 the deposit is stopped and then, pushed forward by the mass remaining on the slope; thus
15 the first inverse faults appear at the front.~~

16 ~~3. Although the frontal part of the deposit is slowed down, the mass continues to propagate on
17 the surface of deposition; thus the front is under a high compressional regime leading to
18 the generation of several inverse faults. Furthermore, shearing takes place at the margins of
19 the deposit, generating strike slip faults. The rear part of the granular flow is still
20 descending along the slope where normal faults are forming because of the extensional
21 state.~~

22 ~~4. Now the mass is completely on the horizontal surface and a thickening of the main body is
23 observe. The moving forward of the mass imply the extension of the back and the
24 formation of normal faults whereas the font is still compressed. The shearing results from
25 the deceleration of the mass.~~

26 ~~5. The mass continues to decelerate on the horizontal surface, the strike slip faults appear at
27 the front of the deposit. These strike slip faults cut both the invers and the normal faults.
28 This type of features is the latest features that appear during all the process of the
29 propagation; they are caused by the progressive deceleration of the mass. Strike slip faults
30 are the surface expression of the shearing at the base of the deposit occurring while the
31 mass is ceasing its movement.~~

1 ~~6. The mass has come to a complete stop.~~

2 ~~Based on this mechanism of propagation, we understand why the features are not randomly~~
3 ~~exposed at the surface of the deposit. This study confirmed that the structures are not~~
4 ~~randomly distributed.~~ As it can be observed in Fig. 6, the inverse faults are present at the

5 frontal part of the deposit, which correspond to the compression-dominated area. Normal
6 faults are mainly observed at the back of the deposit (Figure 6 and Figure 8), which
7 correspond to the extension-dominated area. Finally, strike-slip faults are observed at the
8 back and at the margins of the deposit (Figure 6 and Figure 8). This repartition was also
9 observed in the Blackhawk deposit (Figure 1a) and in a Martian deposit (Figure 1b) (Shea and
10 van Wyk de Vries, 2008). Based on the study of the DEM of Frank Slide deposit and with the
11 filtering technique, the same repartition of the features was observed (Figure 9).

12 **6 Conclusion**

13 The use of 3D dataset, accurate visual inspection and a performing filtering method give
14 crucial information on the motion of granular mass. To summarize:

- 15 1. Three families of faults were highlighted on the surface of the deposit: normal faults,
16 inverse faults and strike-slip faults. We also highlighted that strike-slip faults are
17 present at the back of the deposit.
- 18 2. The identification of the different features allowed identifying three regimes during
19 the propagation of the mass: extensional, compressional and shearing. The extension
20 to real cases of the interpretation of the motion of the granular mass based on
21 laboratory experiments is comforted by the fact that the initial stratigraphy is
22 preserved in both cases and this is an important characteristic of rock avalanche
23 deposits.
- 24 3. The result of the filters on the 3D dataset is a colored point cloud where the slope
25 variations are assigned to a color scale. The method is fast and results into a rapid
26 mapping of the deposit.

27 4. The use of laser scanner and Structure from Motion are two different techniques to get
28 3D dataset. Both are valid and often they result to be complementary.

29 4.5. ~~Even if the simulated roughness is not realistic compared to realistic~~
30 ~~conditions, it gives good insight how the basal roughness influence the motion.~~

31 6. The analogue deposits present similar features as real cases events (Blackhawk and
32 Martian deposits, Figure 1).

1 | ~~5.7.~~ The proposed methodology to map the deposit is fast, easy to use and cheap.

2 | The application of the filtering technique on the deposit of the Frank Slide rock avalanches
3 | gives encouraging results and after some further improvements could be applied in the future
4 | to understand the dynamics of emplacement of historic rock avalanche observing interpreting
5 | their deposit features.

6 | **Acknowledgements**

7 | The authors are grateful to P.-E. Cherix for the design of the laboratory setup and to Martin
8 | Boesinger for his precious help in laboratory. ~~and~~ The authors are also grateful to the Alberta
9 | Geological Service for providing the data of the Frank Slide. Finally, many thanks to the
10 | reviewers for the precious comments.

11

1 **References**

- 2 Adams, T., Grant, C., Watson, H.: Simple algorithm to relate surface roughness to equivalent
3 sand grain roughness, *Int. J. of Mechanical Engineering and Mechatronics*, 1, 2929-2724,
4 2012.
- 5 [Andrade, S., D., van Wyk de Vries, B.: Structural analysis of the early stage of catastrophic](#)
6 [stratovolcano flank-collapse using analogue models. *Bull. Volcanol* 72, 771-789.2010.](#)
- 7 Charrière, M., Humair, F., Froese, C., Jaboyedoff, M., Pedrazzini, A. and Longchamp. C.:
8 From the source area to the deposit: collapse, fragmentation and propagation of the Frank
9 Slide, *GSA Bull.*, 2015.
- 10 Cruden, D.M. and Hungr, O.: The debris of the Frank Slide and theories of rockSlide-
11 avalanche mobility, *Can. J. of earth Sc.*, 23,425-432, 1986.
- 12 Davies, T.R.: Spreading of rock avalanche debris by mechanical fluidization, *Rock*
13 *Mechanics*, 15, 9-24,1982.
- 14 Davies, T.R.H., and McSaveney, M.J.: Runout of dry granular avalanches, *Can. Geotech. J.*,
15 36, 313-320, 1999.
- 16 Davies, T.R.H., McSaveney, M.J.: Runout of rock avalanches and volcanic debris
17 avalanches,. *Proc. Int. Conf. on Fast Slope Movements*, Naples, 2, 2003.
- 18 [Dufresne, A., Davies, T.R: Longitudinal ridges in mass movement deposits. *Geomorphology*](#)
19 [105, p. 171-181, 2009.](#)
- 20 [Dufresne, A.: Granular flow experiments on the interaction with stationary runout path](#)
21 [materials and comparison to rock avalanche events. *Earth Surf. Process. Landforms.*, 37, 14.](#)
22 [2012.](#)
- 23 [Dufresne, A., Prager, C., Bösmeier, A.: Insights into rock avalanche emplacement processes](#)
24 [from detailed morpo-lithological studies oft he Tschirgabt deposit \(Tyrol, Austria\). *Earth*](#)
25 [Surf. Process. Landforms 41, 587-602. 2016.](#)
- 26 Erismann, T.H.: Mechanisms of large landslides, *Rock Mechanics Felsmechanik*, 12(1),15-
27 46, 1979.
- 28 Francis, P.W., Gardeweg, M., O'Callaghan, L.J., Ramirez, C.F. and Rothery, D.A.:
29 Catastrophic debris avalanche deposit of Socompa volcano, north Chile, *Geology*, 14, 600-
30 603, 1985.

- 1 Friedman, S.J., Kwon, G. and Losert, W.: Granular memory and its effect on the triggering
2 and distribution of rock avalanche events, *J. of Geophysical Res.*, 108(B8), 1-11, 2003.
- 3 Gonzalez, R. C., Woods, R. E.: *Digital Image Processing – Sec. Ed.*, Prentice-Hall, Inc., 2002.
- 4 Heim, A.: *Der Bergsturz und Menschenleben*. Fretz und Wasmuth Verlag, Zürich, 218 p.,
5 1932.
- 6 Hsü, K.J.: Catastrophic debris streams (strurzstroms) generated by rockfall, *Geol. Soc. of Am.*
7 *Bul.*, 86, 129-140, 1975.
- 8 Hungr, O., Evans, S.G., Bovis, M., Hutchinson, J.N.: Review of the classification of
9 landslides of the flow type, *Environ. Eng. Geosci.*, VII, 221–238, 2001.
- 10 Iverson, R.M., and Denlinger, R.P.: Flow of variably fluidized granular masses across three-
11 dimensional terrain I. Coulomb mixture theory, *J. of Geophysical Res. B, Solid Earth*,
12 106(B1), 537-552, 2001.
- 13 Kelfoun, K., and Druitt, T.H.: Numerical modelling of the emplacement of Socompa rock
14 avalanche, Chile, *J. of Geophysical Res.*, 110, no. B12, 2005.
- 15 Kumar, L., Skidmore, A.K. and Knowles, E.: Modelling topographic variation in solar
16 radiation in a GIS environment, *Int. J. Geo. Information Sc.*, 11,5, 475-497, 1996.
- 17 Locat P., Couture, R., Leroueil, S., Locat, J., Jaboyedoff, M.: Fragmentation energy in rock
18 avalanches, *Can. Geotech. J.*, 43, 830-851, 2006.
- 19 Longchamp, C., Charrière, M. and Jaboyedoff, M.: Experiments on substratum roughness,
20 grainsize and volume influence on the motion and spreading of rock avalanches, *Pan-Am*
21 *CGS Geotechnical Conference*, 2001.
- 22 [Longchamp, C.: The Propagation of Unconstrained Dry Granular Flows: from Laboratory to](#)
23 [Numerical Modelisation. PhD Thesis, University of Lausanne, Switzerland. 2016.](#)
- 24 Manzella, I.: Dry rock avalanche propagation: unconstrained flow experiments with granular
25 materials and blocks at small scale, PhD thesis, EPFL, 2008,
- 26 Manzella, I., Labiouse, V.: Qualitative analysis of rock avalanches propagation by means of
27 physical modelling of not constrained gravel flows, *Rock Mech. Rock Eng.*, 41 (1), 133–151,
28 2008.

1 Manzella, I., Labiouse, V.: Flow experiments with gravel and blocks at small scale to
2 investigate parameters and mechanisms involved in rock avalanches, Eng. Geol., 109, 146-
3 158, 2009.

4 Manzella, I., and Labiouse, V.: Empirical and analytical analyses of laboratory granular flows
5 to investigate rock avalanche propagation, Landslides, 10, no. 1, 23-36., 2013.

6 McDougall, S., and Hungr, O.: A model for the analysis of rapid landslide motion across
7 three-dimensional terrain, Can. Geotechnical J., 41(6), 1084-1097, 2004.

8 Nicoletti, P.G., and Sorriso-Valvo, M.: Geomorphic controls of the shape and mobility of
9 rock avalanches, Geol. Soc. of Am. Bul., 103(10), 1365-1373, 1991.

10 [Paguican, E. M. R., van Wyk de Vries, B., Lagmay, A. : Hummocks : how they form and how](#)
11 [they evolve in rockslide-debris avalanches. Landslides11. 67-80. 2014.](#)

12 Pedrazzini, A., Froese, C.R., Jaboyedoff, M., Hungr, O., Humair, F.: Combining digital
13 elevation model analysis and run-out modeling to characterize hazard posed by a potentially
14 unstable rock slope at Turtle Mountain, Alberta, Canada. Eng. Geol., 128, 76-94, 2012.

15 Pugazhenti, D., and Pria K.: A quantitative approach for textural image segmentation with
16 median filter, Int. J. of Advancements in Res. & Tech., 2, Issue 4, 2007.

17 Scheidegger, A.E.: On the prediction of the reach and velocity of catastrophic landslides,
18 Rock Mech. and Rock Eng., 5 (4): 231-236, 1973.

19 Shea, T. and van Wyk de Vries, B.: Structural analysis and analogue modeling of the
20 kinematics and dynamics of rockslide avalanches, Geosphere, 4, 657-686, 2008.

21 Van Gassen, W., and Cruden, D.M.: Momentum transfer and friction in the debris of rock
22 avalanches, Can. Geotech. J., 26, 623-628, 1989.

23 van Wyk de Vries, B., Self, S., Francis, P.W., and Keszthelyi, L: A gravitational spreading
24 origin for the Socompa debris avalanche, J. of Vol. and Geothermal Res.,105, p. 225-247.,
25 2001.

26 Westboy, M.J., Brasington, J., Glasser, N.F, Hambrey, M.J. and Reynolds, J.M.: “Structure-
27 from-Motion” photogrammetry: A low-cost, effective tool for geoscience applications,
28 Geomorphology, 179: 300-314, 2012.

29

1 Table 1. Characteristics of the used material.

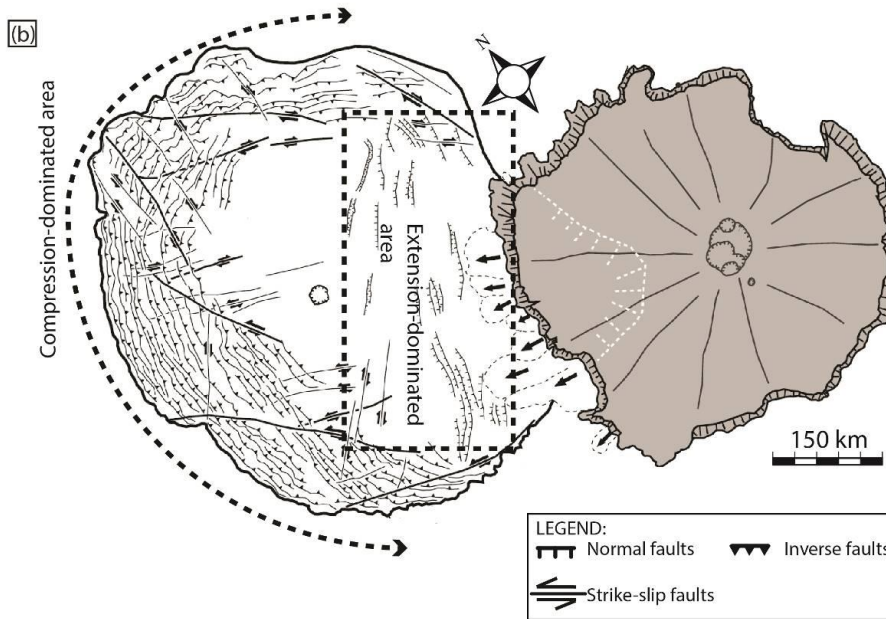
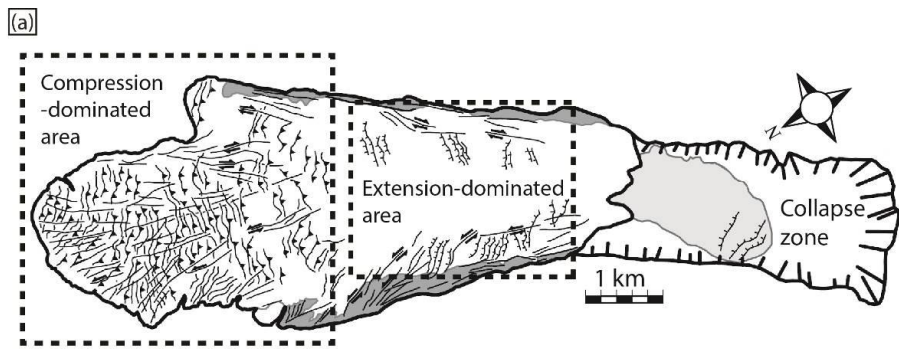
Grading		Mean grainsize(μm)	Range (μm).
Coarse	F10	2605	2830 - 2380
Medium	F36	545	590 - 500
Fine	F120	115	125 – 105
Colored	-	500	-

2

1 Table 2. Characteristics of the different substrata.

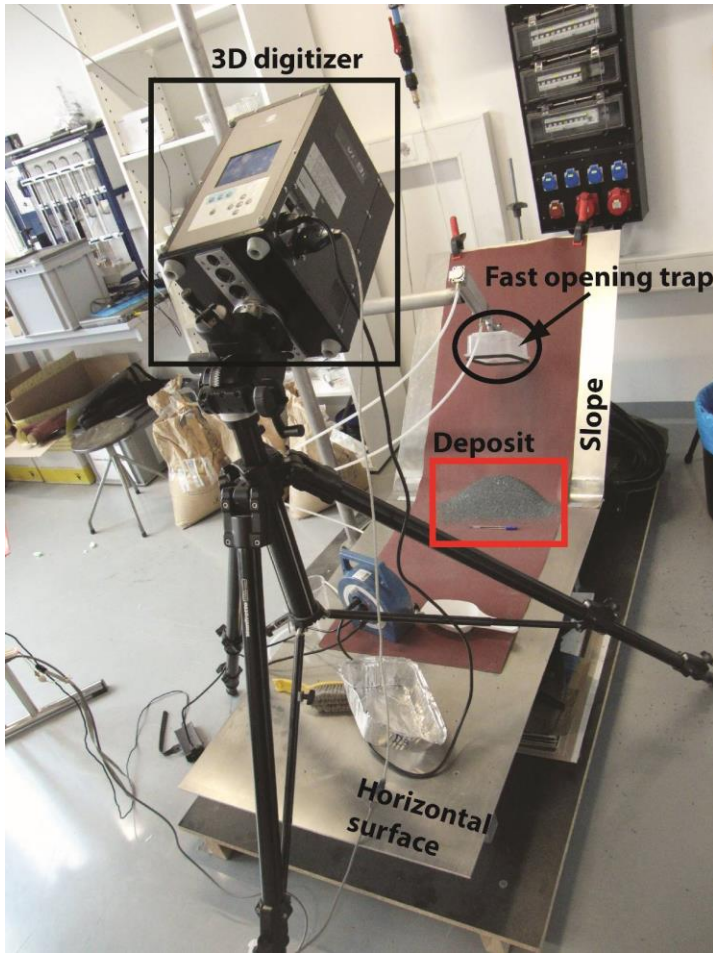
<u>GradingSand</u>	Grit	Grainsize (μm)	<u>Ra (μm)</u>
Coarse	60	269	<u>45.8858.62</u>
	120	125	<u>21.3248.67</u>
Medium	320	46.2	<u>7.8843.17</u>
	600	25.8	<u>4.4039.88</u>
Fine	1200	15.3	<u>2.6134.13</u>
	2500	8.4	<u>1.4333.40</u>
<u>Colored</u>	=	<u>42.5</u>	<u>44.79</u>

2



1
2
3
4
5

Figure 1. (a) Blackhawk deposit and (b) Martian deposit (modified after Shea and van Wyk de Vries, 2008).

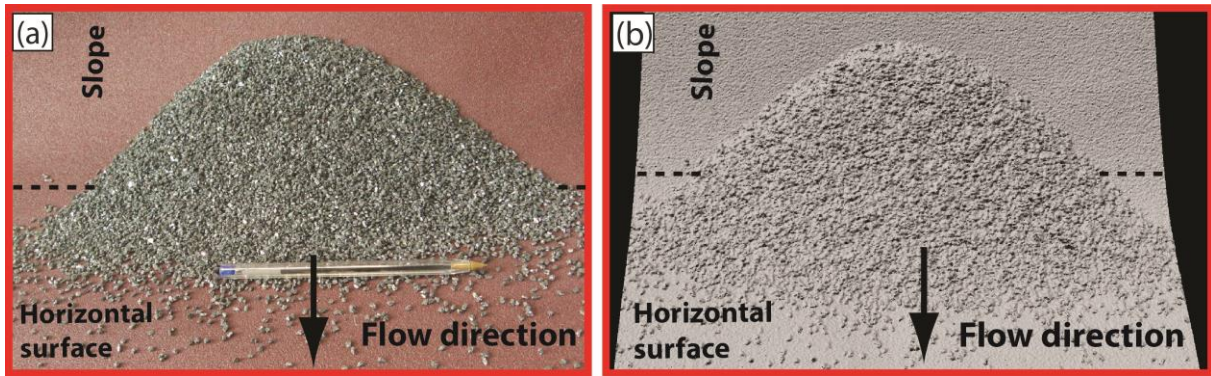


1

2

3 Figure 2. Laboratory setup.

4

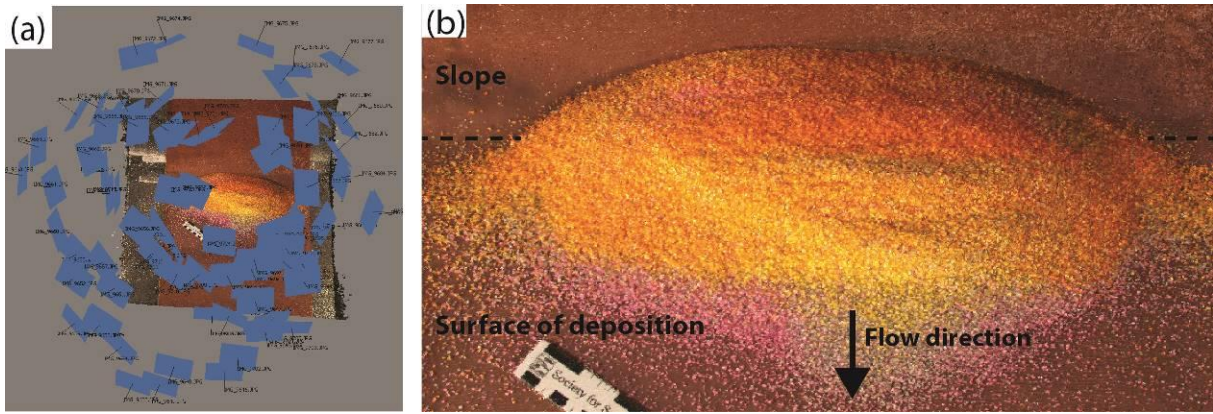


1

2

3 Figure 3: (a) Photography of a deposit of coarse granular material; (b) 3D model of the
4 deposit obtained by 3d laser scanning.

5

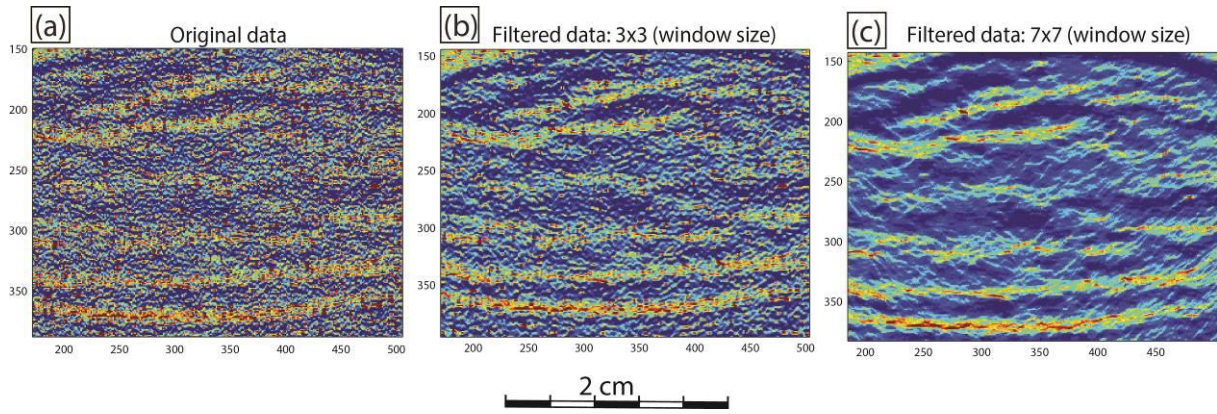


1

2

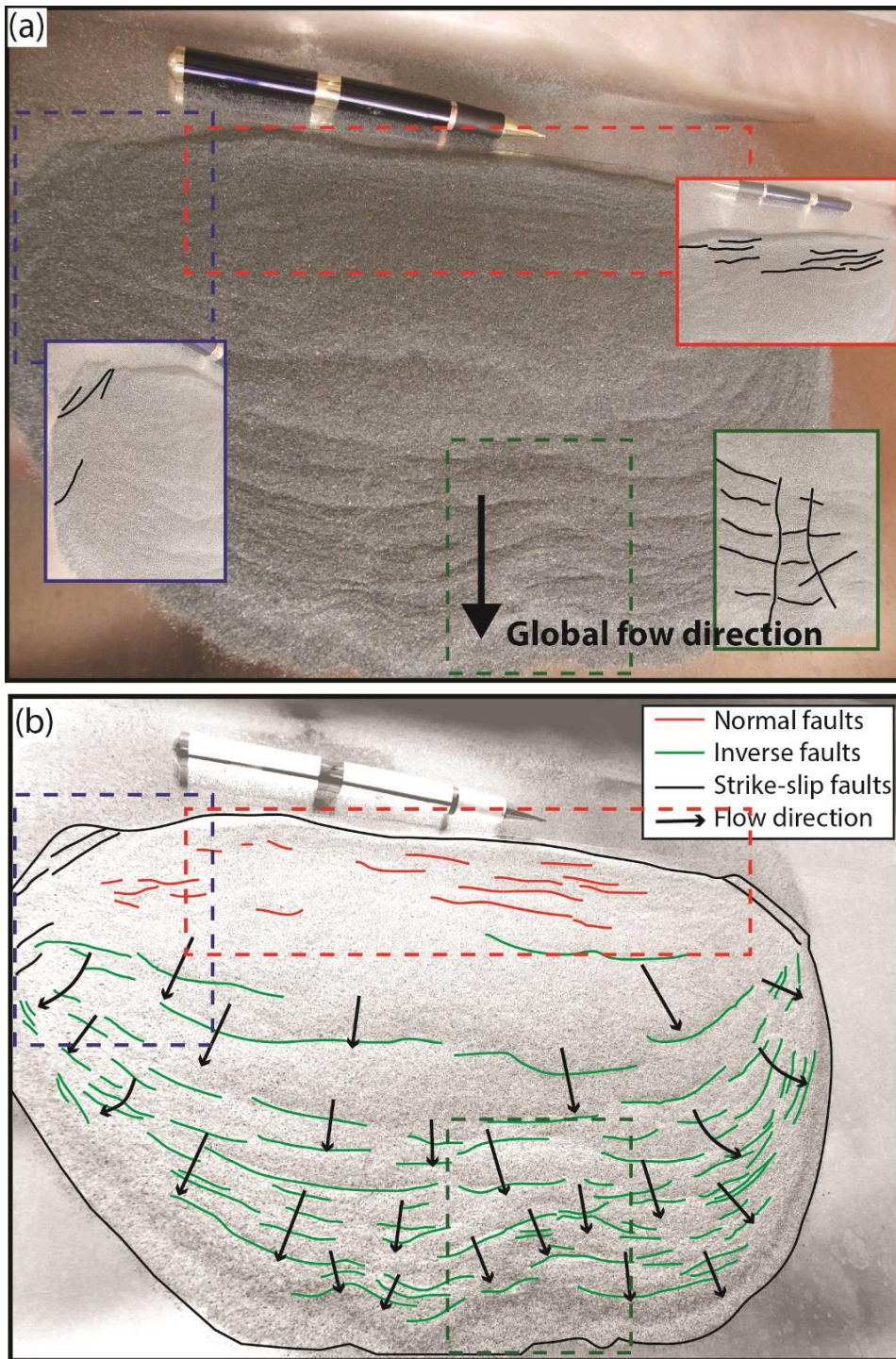
3 Figure 4: (a) View of the different position of the camera to take pictures for structure-from-
4 motion; (b) 3D model obtained with structure-from-motion. Three colored sands were used
5 for this experiment (yellow, grey, pink).

6



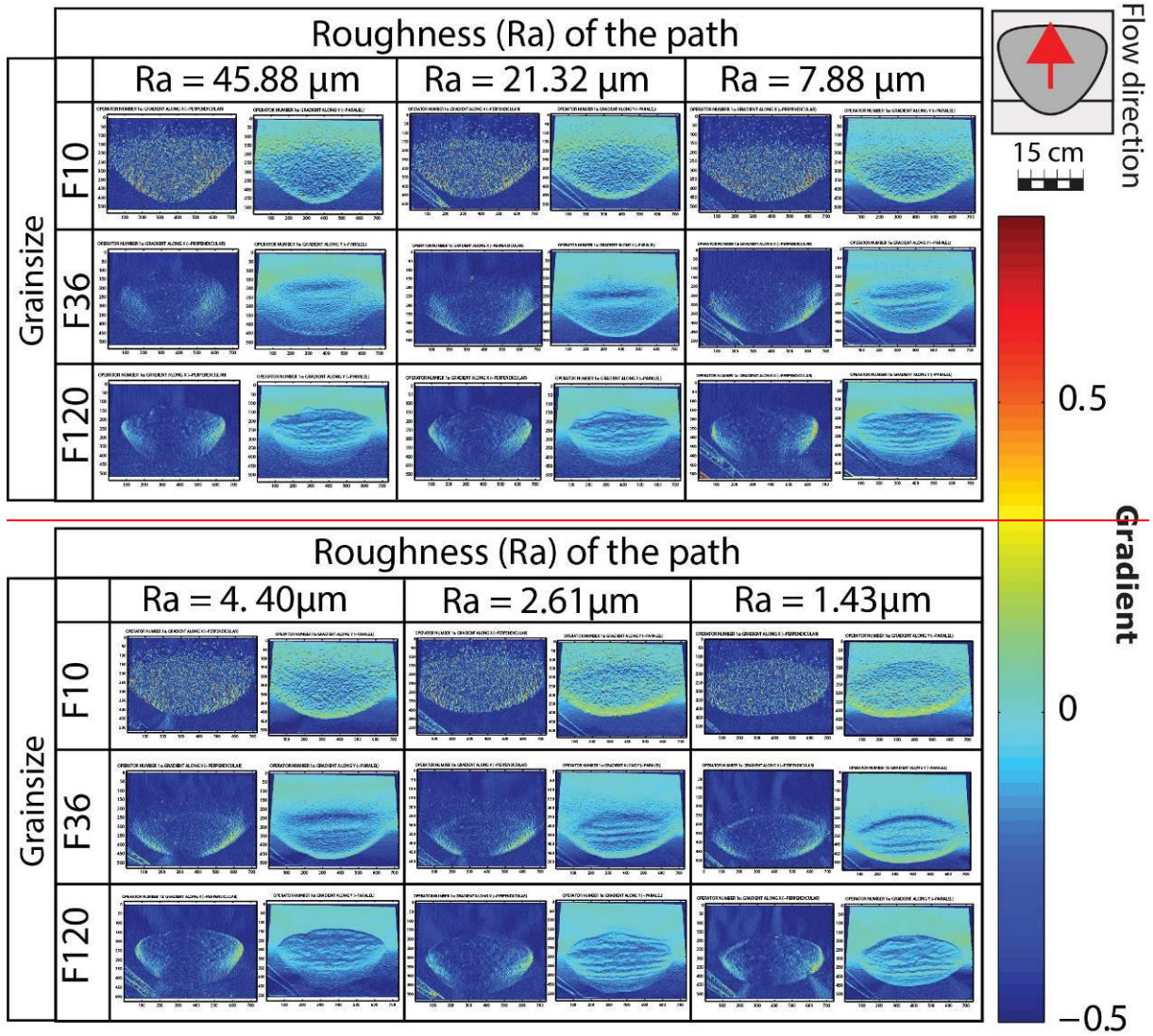
1
2
3
4
5

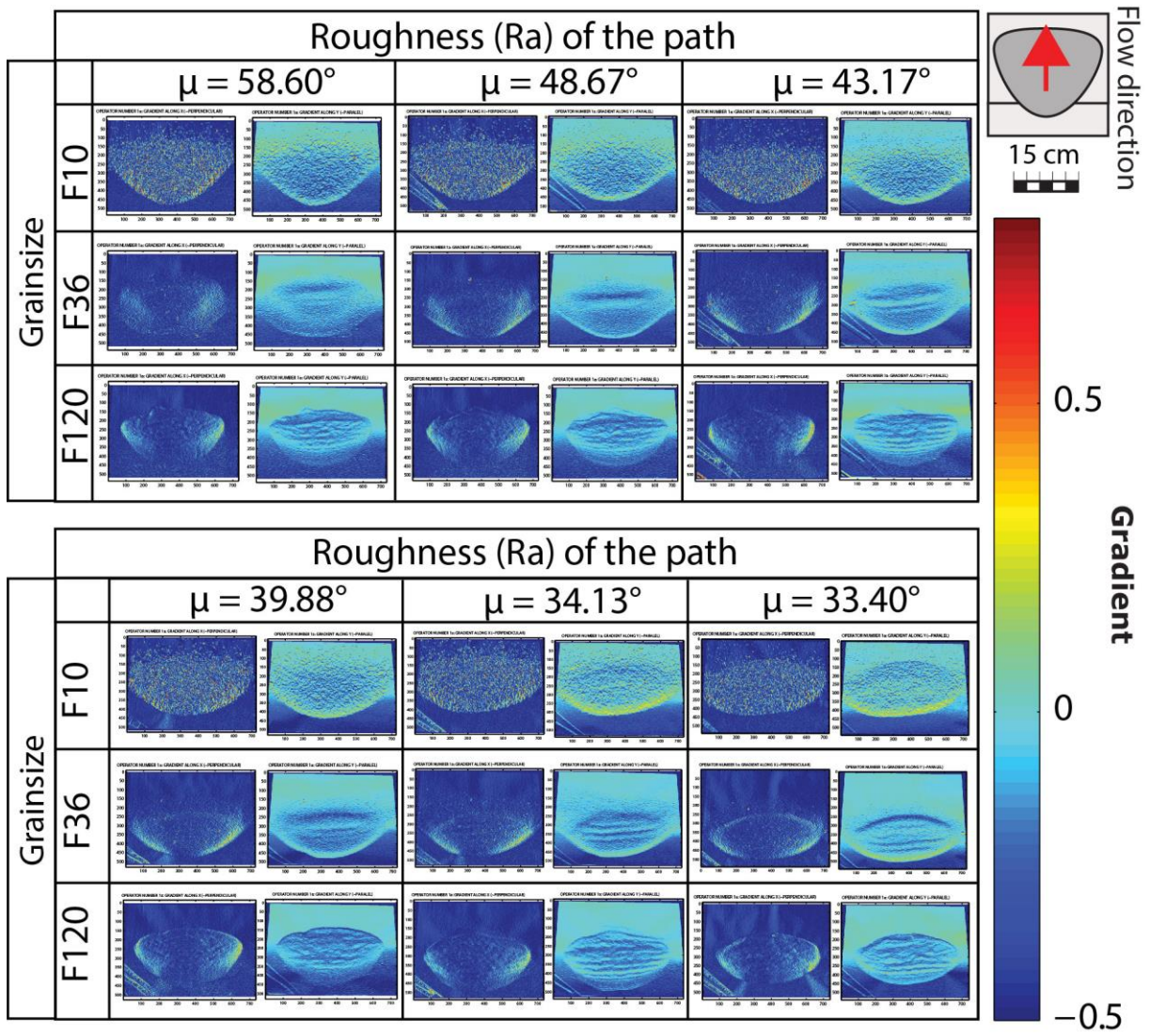
Figure 5: Application of the median filter to remove noises. (a) Original data; (b) Filtered data; (c) with a 3x3 window size; (d) Filtered data with a 7x7 window size.



1
2
3
4
5

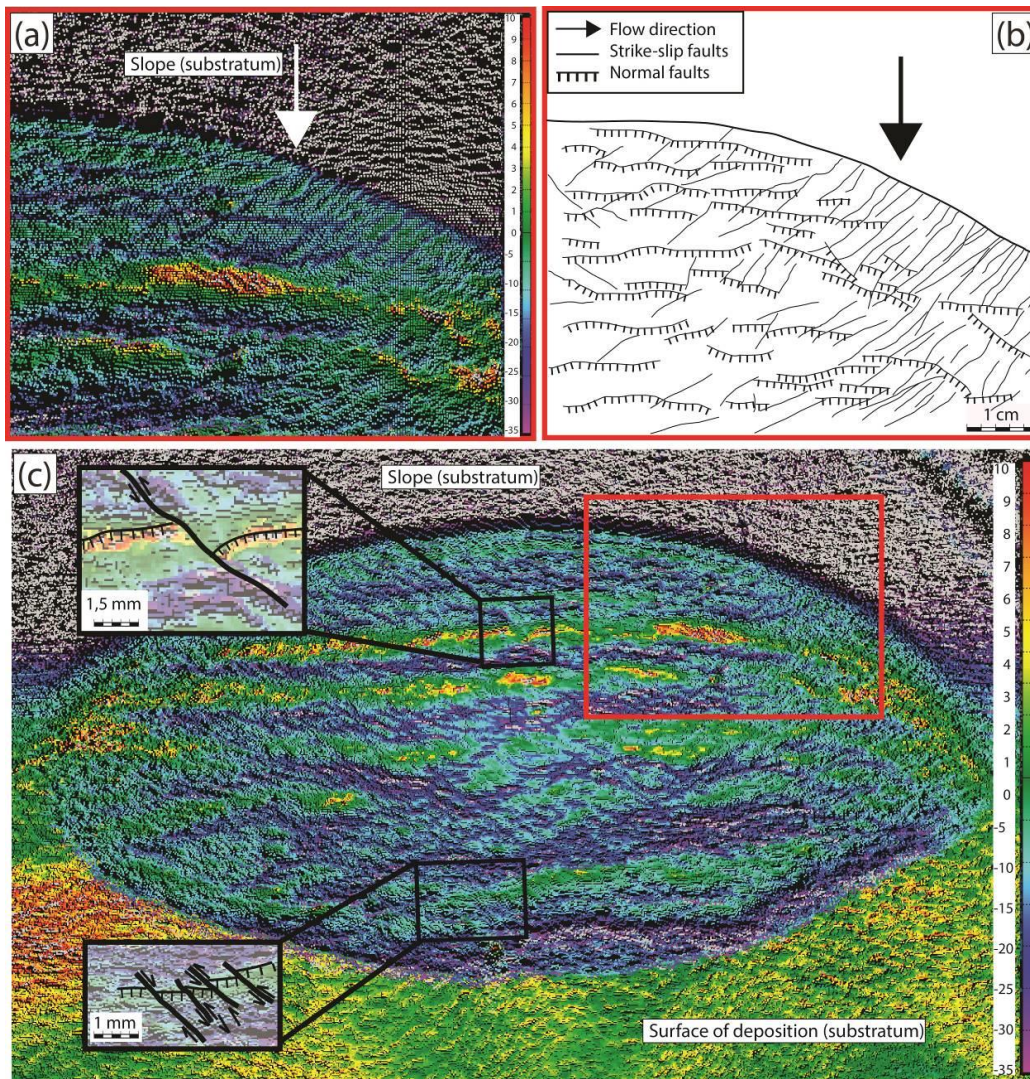
Figure 6: (a) analogue deposit (F120, aluminum substratum), view from the top; (b) result visual inspection and features mapping observed on the deposit surface.





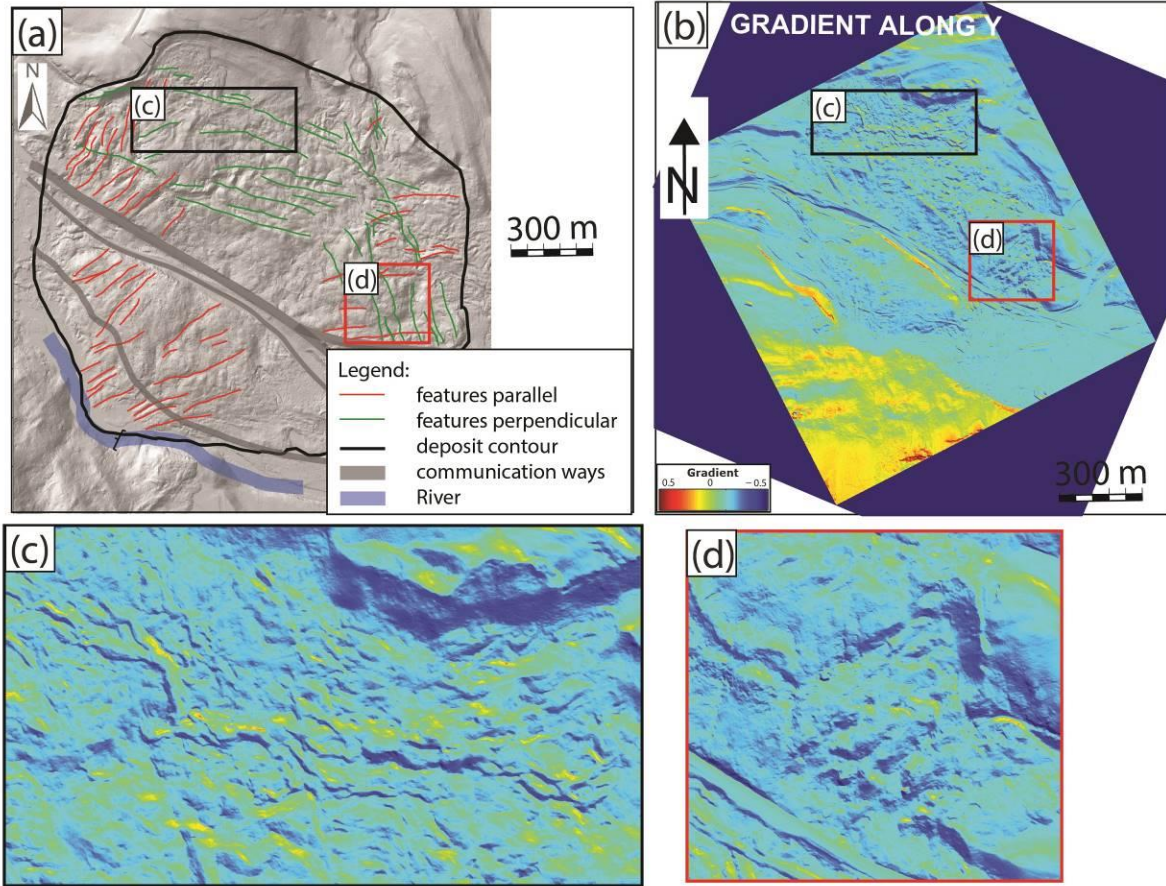
1
2
3
4
5
6

Figure 7: Results of the gradient along X and Y applied to all experiments carried for this research. The best results are obtained with the gradient along Y. The influence of the grainsize and the substratum on the shape of the deposit is clearly observable.



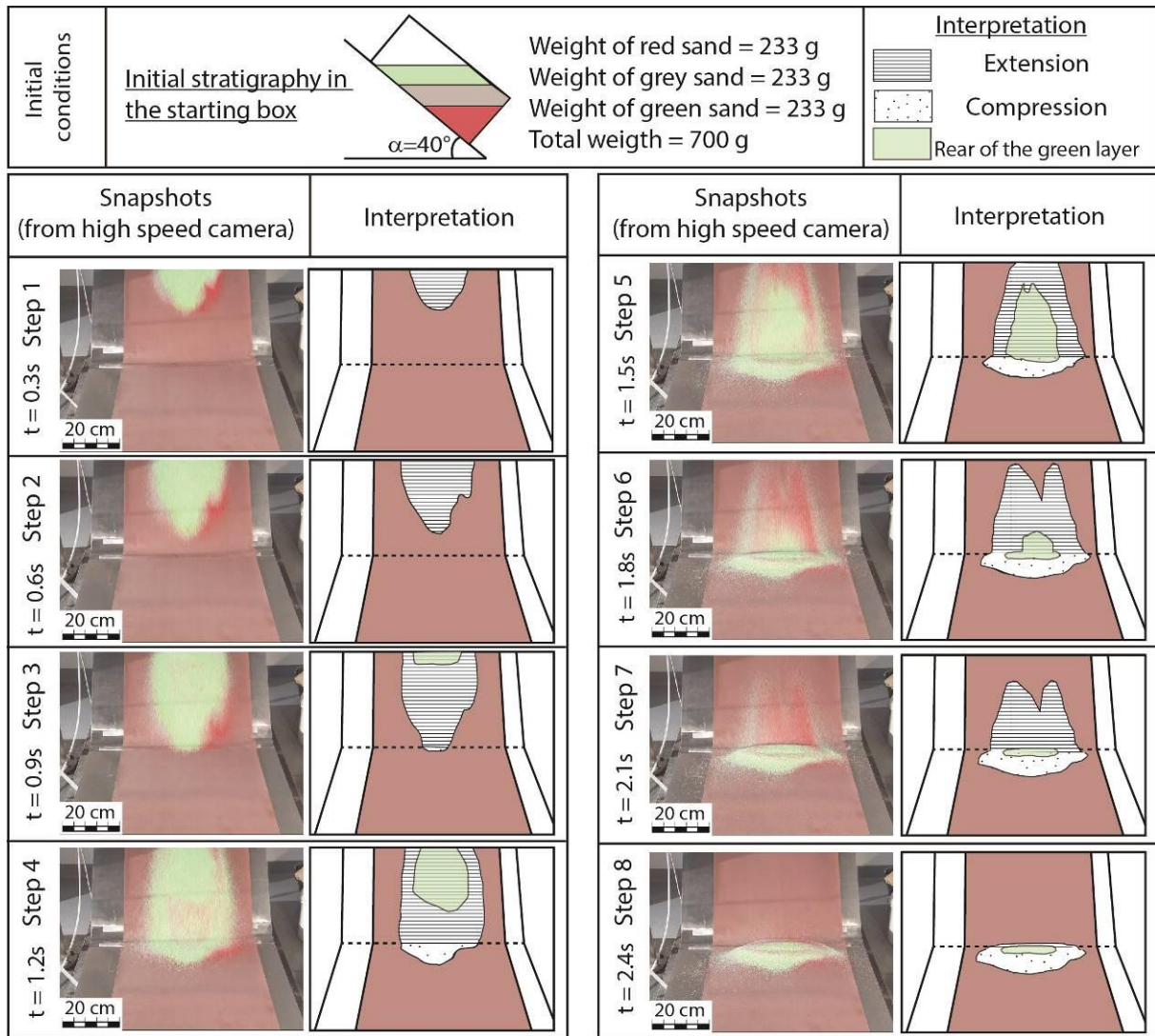
1
2
3
4
5
6

Figure 8: (a) Portion of the back of a deposit after post-processing and (b) detailed mapping of the back of the deposit. Strike-slip faults are numerous at the back, cutting normal faults.(c) the whole result.



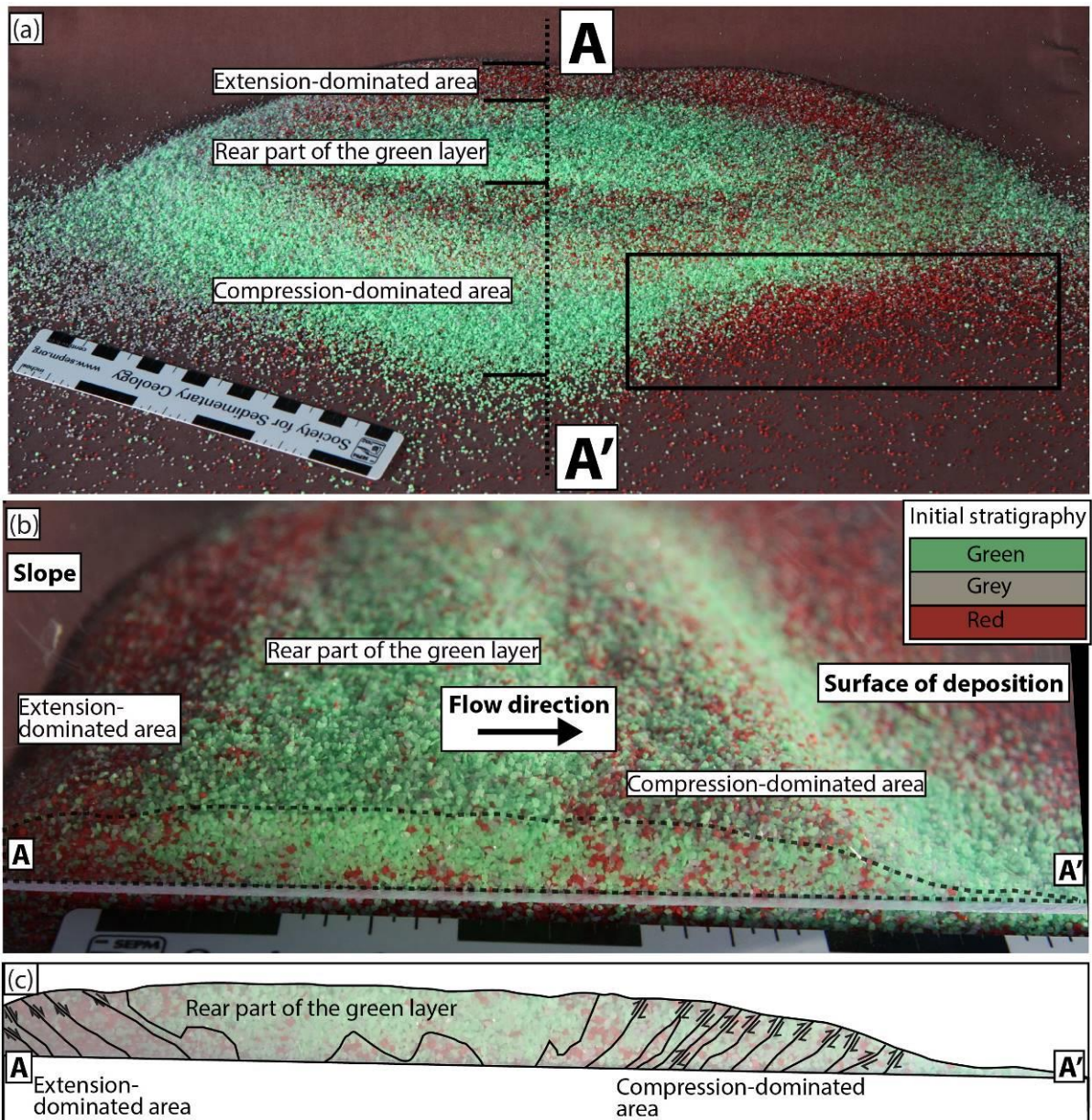
1
2
3
4
5
6

Figure 9: (a) Map of the different features observed on the DEM of Frank Slide deposit; (b) Result of the gradient along Y applied to the DEM of Frank Slide; (c) zoom on features perpendicular to the flow direction; (d) zoom on features parallel to the flow direction.



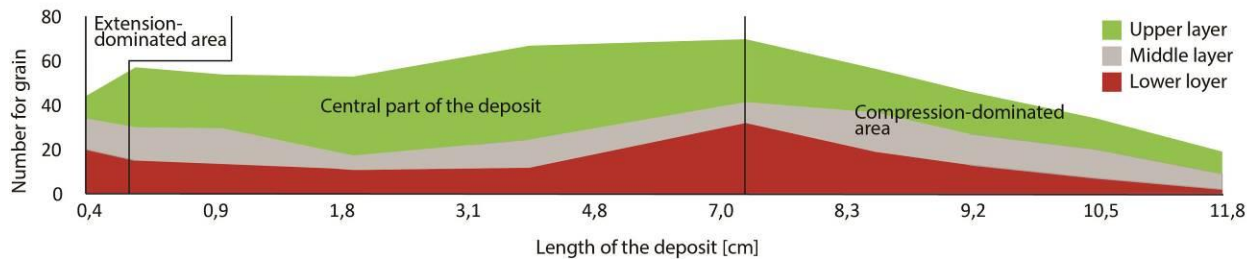
1
2
3
4
5
6

Figure 10: Time laps of an analogue granular flow (0.3 second between each picture). Three colored sand were used during this experiment (red, grey, green). On the left column are the snapshots of the experiment and the right column the interpretation of the flowing mass.



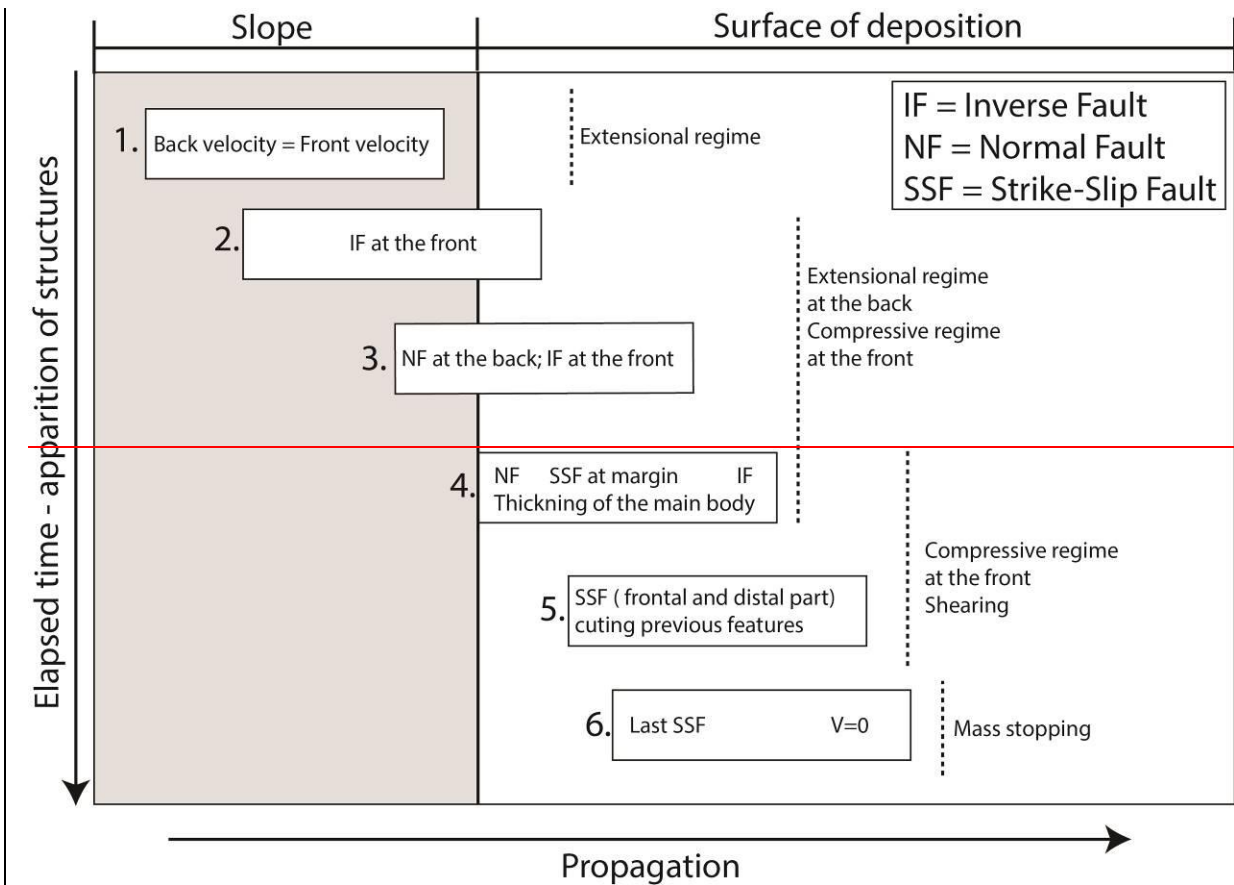
1
2
3
4
5
6

Figure 11: (a) analogue result of the experiment carried with 3 colored sands (Figure 10); (b) cross-section AA' through the center of the analogue deposit; (c) interpretation of the cross-section AA'.



- 1
- 2
- 3
- 4

Figure 12: repartition of the colored sand grains within the deposit.



1
2
3
4

Figure 13: Summarized sketch of the propagation and features appearance of a granular flow in laboratory (modified after Shea and van Wyk de Vries, 2008).